nature immunology

ARTICLES

https://doi.org/10.1038/s41590-020-0782-6

Check for updates

Broad and strong memory CD4+ and CD8+ T cells induced by SARS-CoV-2 in UK convalescent individuals following COVID-19

Yanchun Peng[1,2,23], Alexander J. Mentzer[3,4,5,23], Guihai Liu[2,4,6,23], Xuan Yao[1,2,4,23], Zixi Yin[1,2,23], Danning Dong[2,4,7,23], Wanwisa Dejnirattisai[4,23], Timothy Rostron[8], Piyada Supasa[4], Chang Liu[2,4], César López-Camacho[3,4], Jose Slon-Campos[4], Yuguang Zhao[4], David I. Stuart[2,3,4,9], Guido C. Paesen[3], Jonathan M. Grimes[3,4,9], Alfred A. Antson[10], Oliver W. Bayfield[10], Dorothy E. D. P. Hawkins[10], De-Sheng Ker[10], Beibei Wang[2,4], Lance Turtle[11,12], Krishanthi Subramaniam[12], Paul Thomson[12], Ping Zhang[4], Christina Dold[13,14], Jeremy Ratcliff[4], Peter Simmonds[4], Thushan de Silva[15], Paul Sopp[8], Dannielle Wellington[1,2], Ushani Rajapaksa[2,4], Yi-Ling Chen[1], Mariolina Salio[1], Giorgio Napolitani[1], Wayne Paes[4], Persephone Borrow[4], Benedikt M. Kessler[2,4], Jeremy W. Fry[16], Nikolai F. Schwabe[16], Malcolm G. Semple[12,17], J. Kenneth Baillie[18], Shona C. Moore[12], Peter J. M. Openshaw[19], M. Azim Ansari[4], Susanna Dunachie[4,5], Eleanor Barnes[4,5,20], John Frater[4,5], Georgina Kerr[4], Philip Goulder[4,5], Teresa Lockett[5], Robert Levin[21], Yonghong Zhang[2,6], Ronghua Jing[6], Ling-Pei Ho[1,2,4,20], Oxford Immunology Network Covid-19 Response T cell Consortium*, ISARIC4C Investigators*, Richard J. Cornall[1,4,5], Christopher P. Conlon[2,4,5], Paul Klenerman[4,5,20], Gavin R. Screaton[4,5,20], Juthathip Mongkolsapaya[2,4,20,22], Andrew McMichael[2,4], Julian C. Knight[2,3,4,5], Graham Ogg[1,2,5,20,24] and Tao Dong[1,2,4,24] ✉

The development of severe acute respiratory syndrome coronavirus 2 (SARS-CoV-2) vaccines and therapeutics will depend on understanding viral immunity. We studied T cell memory in 42 patients following recovery from COVID-19 (28 with mild disease and 14 with severe disease) and 16 unexposed donors, using interferon-γ-based assays with peptides spanning SARS-CoV-2 except ORF1. The breadth and magnitude of T cell responses were significantly higher in severe as compared with mild cases. Total and spike-specific T cell responses correlated with spike-specific antibody responses. We identified 41 peptides containing CD4+ and/or CD8+ epitopes, including six immunodominant regions. Six optimized CD8+ epitopes were defined, with peptide–MHC pentamer-positive cells displaying the central and effector memory phenotype. In mild cases, higher proportions of SARS-CoV-2-specific CD8+ T cells were observed. The identification of T cell responses associated with milder disease will support an understanding of protective immunity and highlights the potential of including non-spike proteins within future COVID-19 vaccine design.

COVID-19 is caused by the recently emerged severe acute respiratory syndrome coronavirus 2 (SARS-CoV-2). While the majority of COVID-19 infections are relatively mild, with recovery typically within 2–3 weeks[1,2], a significant number of patients develop severe illness, which is postulated to be related to both an overactive immune response and viral-induced pathology[3,4]. The role of T cell immune responses in disease pathogenesis and longer-term protective immunity is currently poorly defined, but essential to understand in order to inform therapeutic interventions and vaccine design.

Currently, there are many ongoing vaccine trials, but it is unknown whether they will provide long-lasting protective immunity. Most vaccines are designed to induce antibodies to the SARS-CoV-2 spike protein, but it is not yet known if this will be sufficient to induce full protective immunity to SARS-CoV-2 (refs. [5–8]). Studying natural immunity to the virus, including the role of SARS-CoV-2-specific T cells, is critical to fill the current knowledge gaps for improved vaccine design.

For many primary virus infections, it typically takes 7–10 d to prime and expand adaptive T cell immune responses in order to control the virus[9]. This coincides with the typical time it takes for patients with COVID-19 to either recover or develop severe illness. There is an incubation time of 4–7 d before symptom onset and a further 7–10 d before individuals progress to severe disease[10].

A list of affiliations appears at the end of the paper.

Such a pattern of progression raises the possibility that a poor T cell response contributes to SARS-CoV-2 viral persistence and COVID-19 mortality, whereas strong T cell responses are protective in the majority of individuals.

Evidence supporting a role for T cells in COVID-19 protection and pathogenesis is currently incomplete and sometimes conflicting[3,11–14]. To date, there have been few studies analyzing SARS-CoV-2-specific T cell responses and their role in disease progression[15], although virus-specific T cells have been shown to be protective in human influenza infection[16]. In a study of CD4+ and CD8+ T cell responses to SARS-CoV-2 in non-hospitalized convalescent individuals, Grifoni et al.[17] found that all recovered patients established CD4+ responses and 70% established CD8+ memory responses to SARS-CoV-2. SARS-CoV-2-specific CD4+ T cell responses were also frequently observed in unexposed participants in their study, suggesting the possibility of pre-existing cross-reactive immune memory to seasonal coronaviruses. In Singapore, Le Bert et al.[18] found long-lasting T cell immunity to the original SARS coronavirus nucleoprotein (NP) in those who were infected in 2003. These T cells cross-reacted with SARS-CoV-2 NP, and T cells cross-reactive with non-structural proteins 7 and 13 of other coronaviruses were also present in those uninfected with either of the SARS coronaviruses[18].

In the present study, the overall and immunodominant SARS-CoV-2-specific memory T cell responses in patients who had recovered from COVID-19 were evaluated ex vivo using peptides spanning the full proteome of SARS-CoV-2, except ORF1. Epitopes were identified using two-dimensional matrix peptide pools, and CD4+ and CD8+ T cell responses were distinguished. The epitope specificity and human leukocyte antigen (HLA) restriction of the dominant CD8+ T cell responses were defined in ex vivo assays and using in vitro-cultured short-term T cell lines. The ex vivo functions of SARS-CoV-2-specific T cells specific for dominant epitopes were evaluated by their intracellular cytokine production profiles. Broad, and frequently strong, SARS-CoV-2-specific CD4+ and CD8+ T cell responses were seen in the majority of convalescent patients, with significantly larger overall T cell responses in those who had severe compared with mild disease. However, there was a greater proportion of CD8+ T cell compared with CD4+ T cell responses in mild cases, with higher frequencies of multi-cytokine production by matrix (M)- and NP-specific CD8+ T cells.

Results

Study participants. A total of 42 individuals were recruited following recovery from COVID-19, including 28 mild cases and 14 severe cases. In addition, 16 control individuals sampled in 2017–2019, before COVID-19 appeared, were studied in parallel. Supplementary Fig. 1 shows the participant characteristics. No significant differences in gender or age were noted between mild and severe groups. The percentage of oxyhemoglobin saturation in arterial blood (SaO_2)/fraction of inspired O_2 (FiO_2) ratio in severe cases ranged from 4.3 (where 4.5 would be the estimate for an individual with mild disease breathing ambient air) to 1.6, with the patients with critical disease having an estimate of 0.8 (median in severe group = 3.8).

Ex vivo assessment of memory T cell responses specific to SARS-CoV-2. Peripheral blood mononuclear cells (PBMCs) were tested for responses to a panel of 423 overlapping peptides spanning the SARS-CoV-2 proteome except ORF1, using ex vivo interferon-γ (IFN-γ) enzyme-linked immunospot (ELISpot) assays. All overlapping peptides were placed into two two-dimensional peptide matrices. A total of 61 peptide pools were tested, with 29 peptides in the first-dimension pools, as described in Supplementary Table 1. The majority of the participants exhibited SARS-CoV-2 memory T cell responses to at least one of the peptides. The overall distribution, magnitude and breadth of the IFN-γ responses against all SARS-CoV-2 virus peptides are shown in Fig. 1. There was no correlation between the T cell responses and the time that had elapsed from symptom development (Supplementary Fig. 2). No ex vivo IFN-γ-producing SARS-CoV-2-specific T cell responses were observed in healthy volunteers, who were all sampled before any chance of exposure, but in those with appropriate HLA types, T cell responses were observed to influenza virus, Epstein–Barr virus and cytomegalovirus (CMV) using pools of known T cell epitopes, as well as phytohemagglutinin, as positive controls (Supplementary Fig. 3). The breadth and magnitude of the T cell responses varied considerably between individuals. T cell responses were detected against epitopes distributed across a wide variety of virus proteins. Significantly higher-magnitude ($P = 0.002$) and broader ($P = 0.002$) overall T cell responses were observed in severe cases compared with mild cases, in particular for responses to spike ($P = 0.021$ for magnitude; $P = 0.016$ for breadth), membrane ($P = 0.0003$ for magnitude; $P = 0.033$ for breadth), ORF3 ($P < 0.0001$ for magnitude; $P < 0.001$ for breadth) and ORF8 proteins ($P = 0.011$ for magnitude; $P = 0.014$ for breadth) (Fig. 2). Overall, we found that strong and broad T cell memory responses were induced after recovery from COVID-19, and the breadth and magnitude of T cell responses were significantly higher in severe compared with mild cases.

Correlation with spike-specific antibody responses. The relationships between overall and spike-specific T cell responses and spike-specific, receptor-binding domain (RBD)-specific and NP-specific antibody end-point titers (EPTs) were assessed (Fig. 3 and Supplementary Fig. 4). There were significant correlations between: (1) spike-specific antibody titers and both overall T cell responses ($P = 0.0004$; $R = 0.5185$) and spike-specific T cell responses ($P = 0.0006$; $R = 0.505$); (2) RBD-specific antibody titers and both overall T cell responses ($P = 0.0004$; $R = 0.5198$) and spike-specific T cell responses ($P = 0.0004$; $R = 0.5189$); and (3) NP-specific antibody titers and both overall T cell responses ($P = 0.0015$; $R = 0.4738$) and spike-specific T cell responses ($P = 0.007$; $R = 0.412$). However, there was no significant association between NP-specific antibody titers and NP-specific T cell responses ($P = 0.067$; $R = 0.286$) (Supplementary Fig. 4). Moreover, significantly higher levels of spike, RBD and NP EPTs were observed in severe cases compared with mild cases (Fig. 3d). It was noted that some individuals had low RBD-specific antibodies (Fig. 3b), yet had detectable spike-specific antibodies (Fig. 3a), suggesting that antibodies were able to target non-RBD regions of spike. This is under further investigation. Thus, total and spike-specific T cell responses were found to be correlated with spike-specific antibody responses.

Distribution of SARS-CoV-2-specific CD4+ and CD8+ memory T cell responses. Having identified overall T cell responses to SARS-CoV-2 peptides, the responses detected against positive peptide pools were characterized by flow cytometry for peptide recognition by CD4+ or CD8+ T cell subsets and for intracellular production of IFN-γ, tumor necrosis factor-α (TNF-α) and interleukin-2 (IL-2) after stimulation (Fig. 4a,b and Supplementary Fig. 5). A greater proportion of the T cell responses to spike ($P = 0.0268$) and M/NP ($P = 0.02$) were contributed to by CD8+ T cells in those with mild disease compared with those with severe disease (Fig. 4c and Supplementary Fig. 6a). Differential subsets of SARS-CoV-2-specific T cells therefore associate with clinical outcome.

Evaluation of the polyfunctionality of T cells responding to SARS-CoV-2 peptides. Multi-cytokine analysis revealed patterns of IFN-γ, TNF and IL-2 production by CD4+ and CD8+ T cells in both mild and severe cases (Fig. 5a). For 22 individuals tested, both CD4+ and CD8+ antigen-specific T cells produced at least one of these three cytokines and others in combination. CD8+ but not CD4+ T cells targeting different virus proteins showed different

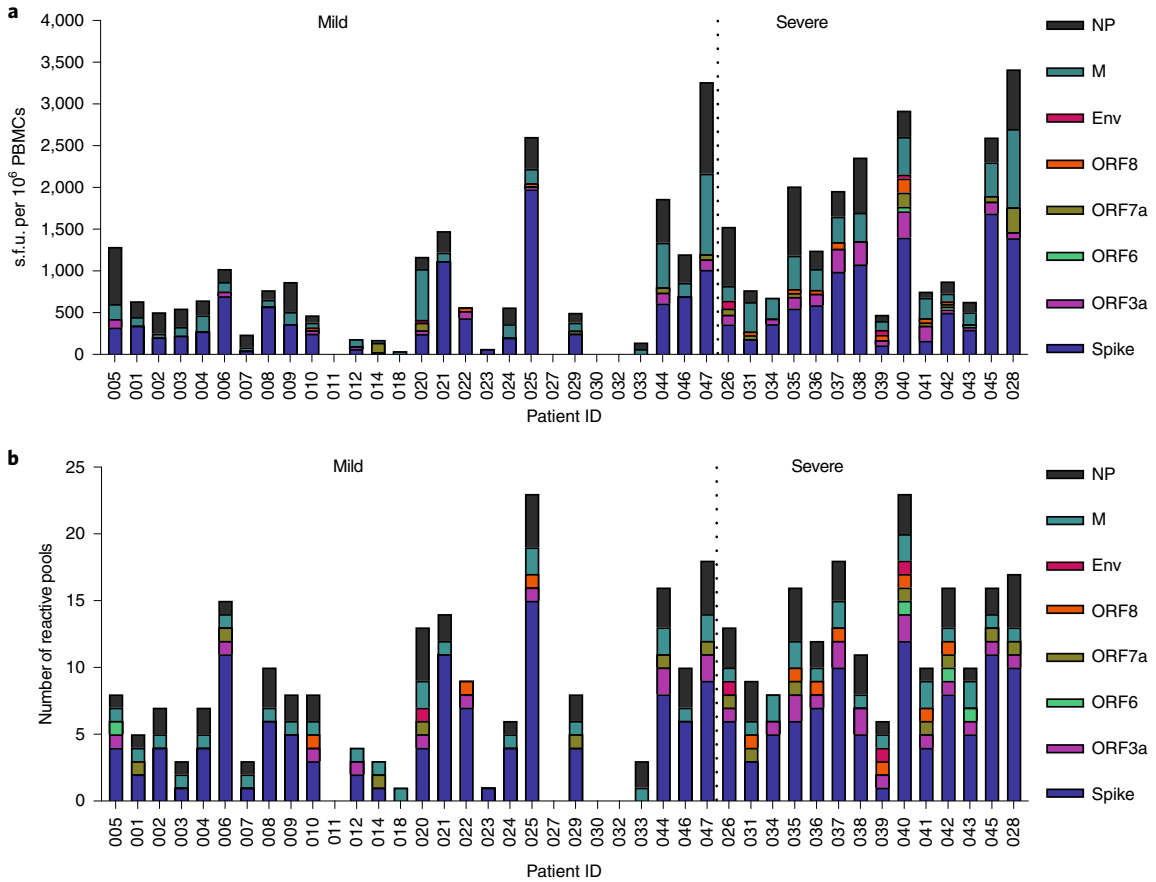

Fig. 1 | Memory T cell responses specific to SARS-CoV-2 virus proteins in 42 convalescent patients infected with SARS-CoV-2. Of the 42 patients studied, 28 had mild symptoms while 14 showed severe symptoms. PBMCs were isolated and IFN-γ production was detected by ELISpot after incubation with SARS-CoV-2 peptides. **a**, Magnitude of IFN-γ T cell responses for each individual. Each bar shows the total T cell responses of each individual specific to all of the SARS-CoV-2 protein peptides tested. Each colored segment represents the source protein corresponding to peptide pools eliciting IFN-γ T cell responses. **b**, Breadth of T cell responses for each individual. The breadth of T cell responses was calculated by the number of peptide pools in the first-dimension ($n=29$) cells that responded to spot-forming units. The experiments were repeated in 35 participants where sample availability permitted. Env, envelope protein.

cytokine profiles, with the M/NP-specific CD8$^+$ T cells showing wider functionality than T cells targeting spike protein ($P=0.0231$; Fig. 5b and Supplementary Fig. 6b). Furthermore, there were a greater proportion of multifunctional M/NP-specific CD8$^+$ T cells compared with spike-specific T cells in those who had mild disease ($P=0.0037$), but not in those who had severe disease ($P=0.3823$). In contrast with observations seen in influenza virus infection[19], we did not observe significant differences in the cytotoxic potential (as indicated by expression of the degranulation marker CD107a) in patients with mild and severe disease (Fig. 5c) and we observed very few CD107a$^+$CD4$^+$ T cells overall, suggesting that cytotoxic CD4$^+$ T cells might not be a major contributor to virus clearance.

Identification of SARS-CoV-2-specific T cell peptides containing epitopes. IFN-γ ELISpot assays were performed with candidate peptides identified from the two-dimensional matrix analysis in 34 participants. A total of 41 peptides containing SARS-CoV-2 T cell epitope regions were recognized by convalescent individuals who had COVID-19: 18 from spike, ten from NP, six from membrane and seven from ORF proteins. Strikingly, six dominant 18-mer peptides were recognized by six or more of the 34 participants tested (Table 1). NP-16 was recognized by 12 out of 34 (35%) participants tested and contained at least two epitopes that were recognized by either CD4$^+$ T or CD8$^+$ T cells.

M-24 was recognized by 16 out of 34 participants (47%) tested and contained one or more CD4$^+$ T cell epitopes. Peptide M-20 was recognized by 11 out of 34 participants tested (32%) and contained one or more CD4$^+$ T cell epitopes. Three dominant spike peptides were also identified, with S-34 recognized by ten out of 34 participants (29%) containing both CD4$^+$ and CD8$^+$ T cell epitopes, and a further two spike peptides (S-151 and S-174) were recognized by eight and six out of 34 participants, respectively (24 and 18%), both containing CD4$^+$ T cell epitopes.

Those dominant responses were further confirmed by ex vivo assays and using cultured short-term T cell lines. Supplementary Fig. 7 illustrates examples of fluorescence-activated cell sorting plots from intracellular cytokine staining (ICS) when short-term T cell lines were stimulated with single peptides containing epitopes. CD4$^+$ T cells elicited strong responses against dominant spike peptides and M peptides, whereas cells targeting two NP-dominant peptides were CD8$^+$ T cells. The optimum epitopes within the long peptides recognized by dominant CD8$^+$ T cells, and their HLA restriction matched to the donor's HLA type, were predicted using the Immune Epitope Database analysis resource (http://tools.iedb.org/mhci). The best-predicted epitope sequences are shown in Supplementary Table 2.

A set of previously defined SARS epitopes[20] with identical sequences to SARS-CoV-2 were also tested by ELISpot assay

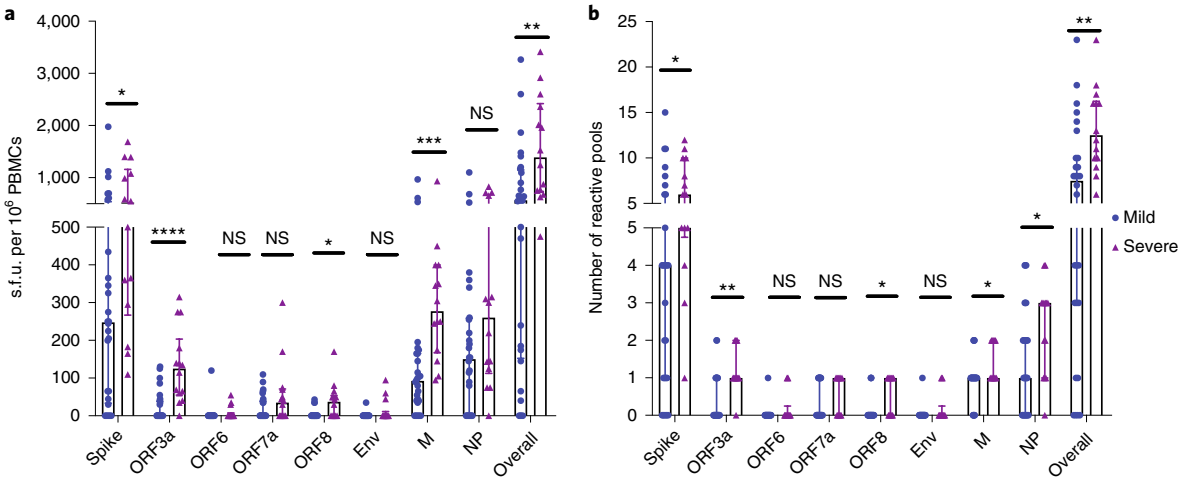

Fig. 2 | Comparison of the magnitude and breadth of T cell responses specific to each viral protein between convalescent patients with mild symptoms and those with severe symptoms. PBMCs were isolated and IFN-γ production was detected by ELISpot after incubation with SARS-CoV-2 peptides. **a**,**b**, Magnitude (**a**) and breadth (**b**) of T cell responses against each viral protein between those with mild symptoms ($n=28$) and those with severe symptoms ($n=14$). *P* values were as follows: overall: $P=0.002$ for magnitude; $P=0.002$ for breadth; spike: $P=0.021$ for magnitude; $P=0.016$ for breadth; membrane: $P=0.0003$ for magnitude; $P=0.033$ for breadth; ORF3a: $P<0.0001$ for magnitude; $P=0.001$ for breadth; ORF8: $P=0.011$ for magnitude; $P=0.014$ for breadth. Data are presented as medians with interquartile ranges. The Mann–Whitney *U*-test was used for the analysis and two-tailed *P* values were calculated. $^{*}P<0.05$; $^{**}P<0.01$; $^{***}P<0.001$; $^{****}P<0.001$. NS, not significant.

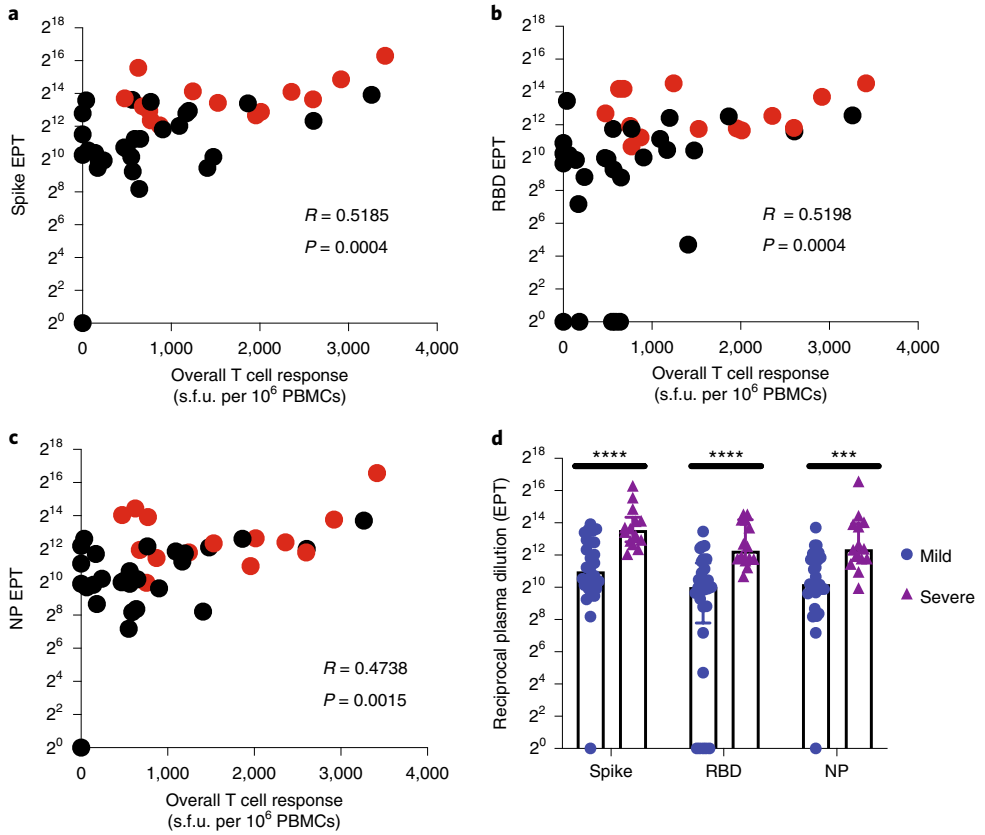

Fig. 3 | Correlation of T cell responses against SARS-CoV-2 with spike-, RBD- and NP-specific antibody responses. a–**c**, Spike (**a**), RBD (**b**) and NP EPTs (**c**) in association with overall T cell responses. Red and black data points represent patients with severe and mild symptoms, respectively. $n=42$. Spearman's rank correlation coefficients (*R*) are shown. **d**, Comparison of spike EPTs ($P<0.0001$), RBD EPTs ($P<0.0001$) and NP EPTs ($P=0.0004$) for patients with mild symptoms ($n=28$) versus severe symptoms ($n=14$). Data are presented as medians with interquartile ranges and a Mann–Whitney *U*-test was used for comparison. Two-tailed *P* values were calculated. $^{***}P<0.001$; $^{****}P<0.0001$.

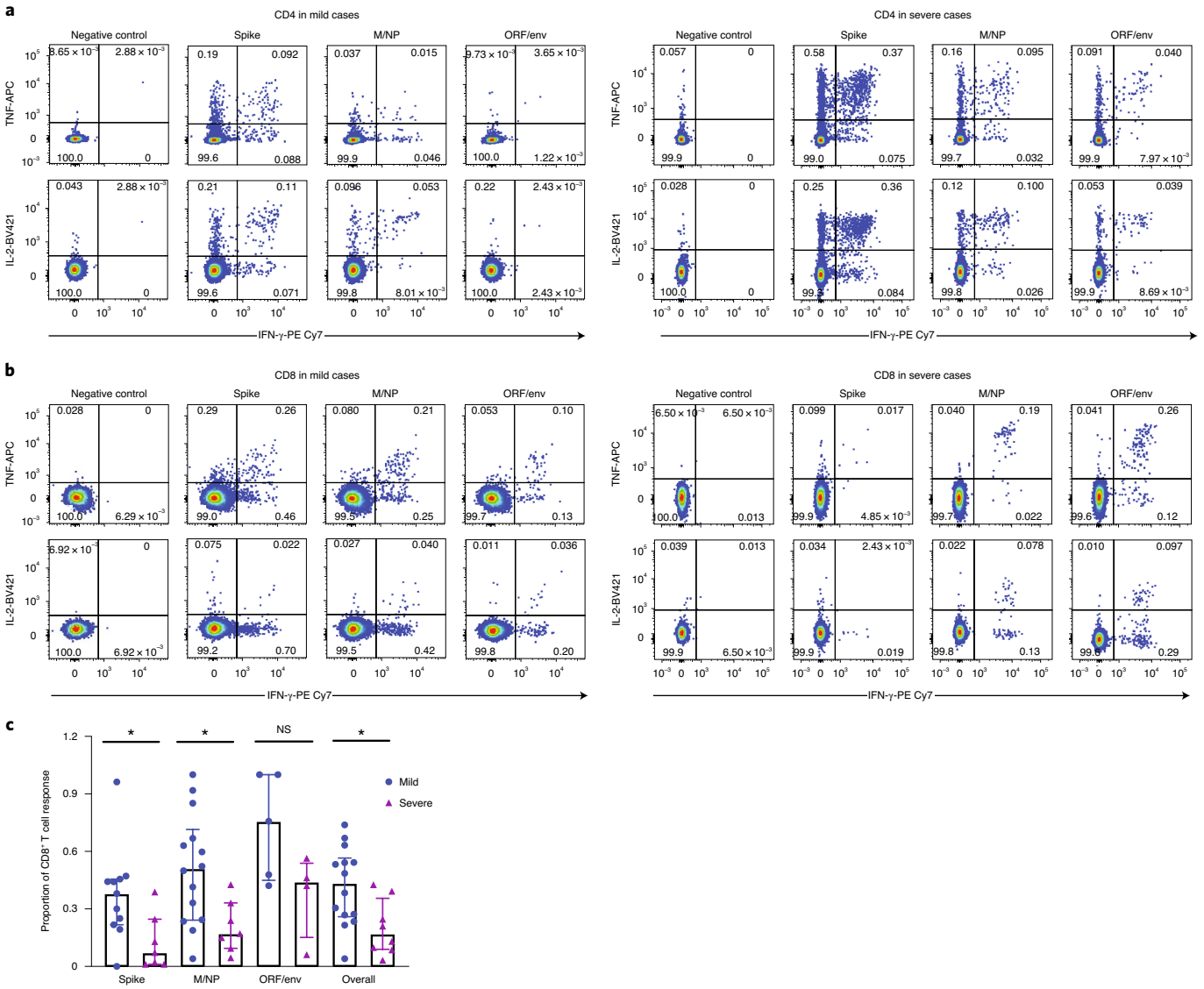

Fig. 4 | Distribution of SARS-CoV-2-specific CD4⁺ and CD8⁺ memory T cell responses. Cytokine-producing T cells were detected by ICS after incubation with SARS-CoV-2 peptides. **a**,**b**, Flow cytometric plots representing CD4⁺ T cells (**a**) and CD8⁺ T cells (**b**) expressing IFN-γ (*x* axis), TNF (*y* axis) and/or IL-2 (*y* axis) upon stimulation with the respective SARS-CoV-2 peptide pools in examples of mild (left) and severe cases (right). **c**, Comparison of the relative proportion of SARS-CoV-2 peptide-pool-reactive CD8⁺ T cells between mild (spike, $n=11$; M/NP, $n=14$; ORF/Env, $n=5$; overall: $n=14$) and severe cases (spike, $n=7$; M/NP, $n=7$; ORF/Env, $n=4$; overall, $n=8$). *P* values were as follows: $P=0.0268$ (spike); $P=0.02$ (M/NP); $P=0.0159$ (overall). The SARS-CoV-2 peptide-pool-reactive CD4⁺ or CD8⁺ T cells were identified with at least one of the three cytokines (IFN-γ, TNF and IL-2) detected. Data are shown as medians with interquartile ranges. The Mann–Whitney *U*-test was used for the analysis. Two-tailed *P* values were calculated. $^*P<0.05$.

(Supplementary Table 3). Most of those peptides did not elicit any positive responses in 42 individuals who had recovered from COVID-19, apart from two NP epitope peptides (N-E-3 (MEVTPSGTWL) and N-E-11 (LLNKHIDAYKTFPPTEPK)) and one spike epitope peptide (S-E-19; QLIRAAEIRASANLAATK) . N-E-11, which is identical to peptide NP-51, shares the sequence with two other known HLA-A*0201-restricted SARS epitopes (N-E-1 (ILLNKHID) and N-E-5 (ILLNKHIDA)). Interestingly, one of the responders to this peptide did not carry the HLA-A*0201 allele (Table 1), indicating that this peptide may contain a different SARS-CoV-2 epitope presented by a different HLA molecule. Whereas these NP epitopes are targeted by CD8⁺ T cells, we also detected a CD4⁺ T cell response targeting SARS spike epitope S-E-19, which spans between the overlapping peptides of S-203 and S-204. This peptide is known to be presented by HLA-DRB1*0401 in SARS infection.

The optimum peptide sequences and their HLA restrictions were confirmed by generating short-term T cell lines and clones, which were tested in ELISpot assays by co-culturing with peptide-loaded HLA-matched and -unmatched immortalized B lymphoblastoid cell lines, as previously described[21]. In total, six CD8⁺ T cell epitopes restricted by HLA-A*0101, -A*0301, -A*1101, -B*0702, -B*4001 and -B*2705 were confirmed (Table 2). HLA–peptide pentamers were synthesized comprising five peptides bound to the appropriate HLA class I molecules. T cell staining was verified by flow cytometry (Fig. 6) and their phenotypes were determined (Fig. 7). A pentameric HLA-A*0201 with the spike epitope reported by Shomuradova et al.[22], was synthesized. Only one out of six HLA-A*0201-positive donors showed detectable staining, but at a very low frequency. The majority of pentamer-stained SARS-CoV-2-specific CD8⁺ T cells exhibited central memory ($20.7\pm8.4\%$) or effector memory phenotypes ($50.3\pm13.3\%$) (Fig. 7) and early (CD27⁺CD28⁺; $43.8\pm20.9\%$)

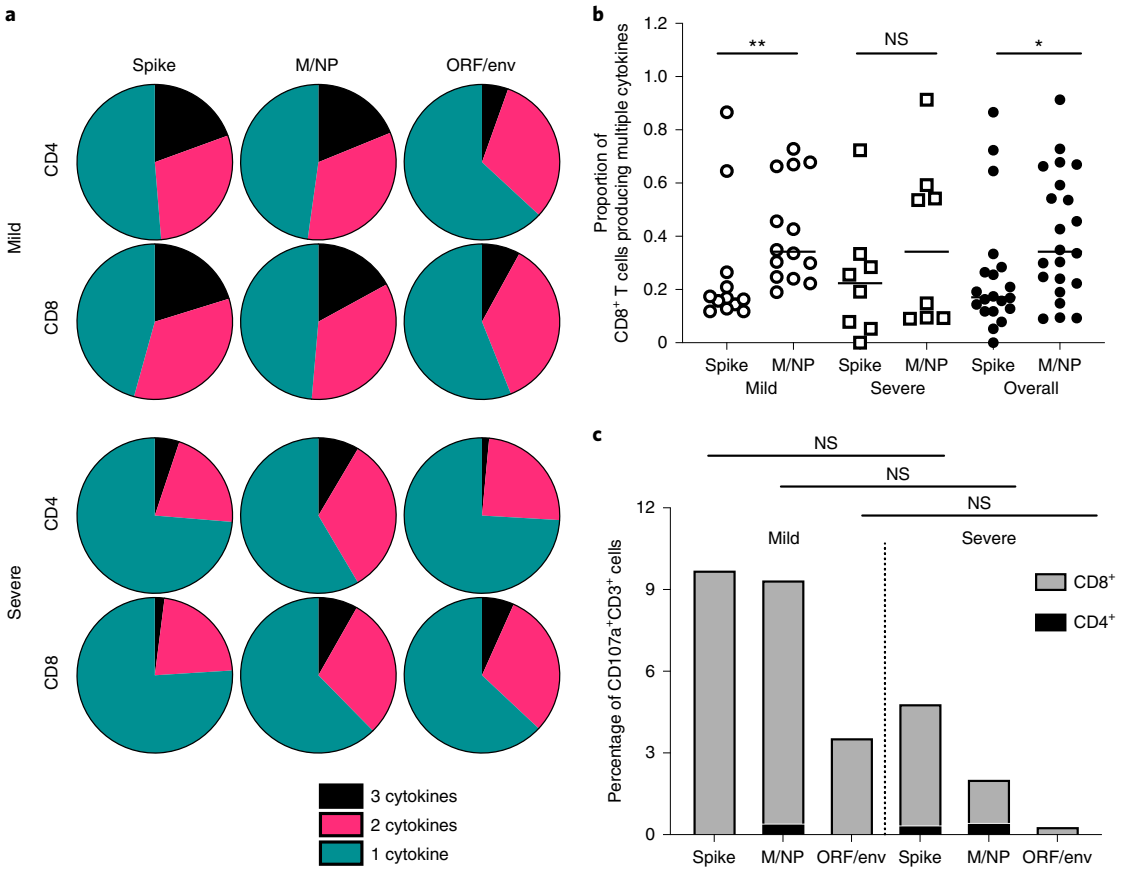

Fig. 5 | Cytokine profile of SARS-Cov-2-specific T cells. The cytokine production of SARS-Cov-2-specific T cells was assessed by ICS after incubation with SARS-CoV-2 peptides. **a**, Pie charts representing the relative proportions of spike-, M/NP- and ORF/env-specific CD4+ and CD8+ T cells producing one (green), two (pink) or three cytokines (black) (out of IFN-γ, TNF and IL-2). **b**, Comparison of the frequency of multifunctional CD8+ T cells targeting spike and M/NP. The open circles and squares represent T cell responses in mild cases and severe cases, respectively. *P* values are as follows: $P = 0.0037$ (mild); $P = 0.3823$ (severe); $P = 0.0231$ (overall). **c**, Relative frequencies of CD4+ and CD8+ T cells expressing CD107a after antigen stimulation. The data shown are from 14 patients with mild symptoms and eight patients with severe symptoms. The Mann–Whitney *U*-test was used for the analysis. Two-tailed *P* values were calculated. $^*P < 0.05$; $^{**}P < 0.01$.

or intermediate ($CD27^+CD28^-$; $49.3 \pm 21.0\%$) differentiation phenotypes. Overall, multiple peptides containing epitopes and immunodominant regions were defined from 42 individuals who had recovered from COVID-19. The regions were located in the majority of SARS-CoV-2 structural and non-structural proteins, including spike, M, NP and ORF proteins, with CD8+ T cells exhibiting central memory and effector memory phenotypes.

Discussion

This study demonstrates the presence of robust memory T cell responses specific for SARS-CoV-2 in the blood of donors who have recovered from COVID-19. The broader and stronger SARS-CoV-2-specific T cell responses in patients who had severe disease may be the result of higher viral loads and may reflect a poorly functioning early T cell response that failed to control the virus, in addition to other factors such as direct virus-induced pathology associated with larger viral inoculums or poorer innate immunity. Alternatively, it is possible that the T cell response was itself harmful and contributes to disease severity. Consistent with recent reports from Grifoni et al.[17] and Sekine et al.[23], a particularly high frequency of spike protein-specific CD4+ T cell responses was observed in patients who had recovered from COVID-19. This is very similar to influenza virus infection, where viral surface hemagglutinin elicited mostly CD4+ T cell responses, whereas the majority of CD8+ T cell responses were specific to viral internal proteins[24]. Understanding the roles of different subsets of T cells in protection or pathogenesis is crucial for the prevention and treatment of COVID-19. The timing and strength of the first T cell responses could be critical in determining this balance at an early stage of the infection.

Among the 41 peptides containing T cell epitopes that were identified in this study, six immunodominant epitope groups (peptides) were frequently targeted by T cells in many donors, including three in spike protein (29, 24 and 18%), two in membrane protein (32 and 47%) and one in NP (35%). The immunodominant peptide regions identified here may include multiple epitopes restricted by different HLAs (both class I and II, such as S-34 and NP-16), with immunodominance preferences imposed by the antigen-processing pathways. Whether or not these dominant responses play a role in immune protection merits further investigation in larger prospective cohorts.

A higher proportion of CD8+ T cell responses was observed in mild disease, suggesting a potential protective role of CD8+ T cell responses in mild disease or a pathogenic role of CD4+ T cell responses in severe disease, which merits further investigation.

The majority of pentamer-binding CD8+ T cells were effector memory and central memory with early and intermediate differentiation phenotypes, with functional potential on antigen re-exposure. Because the number of donors studied was limited and they would probably show diverse T cell receptors, peptide–major histocompatibility complex (MHC) affinities and antigen

Table 1 | Peptides containing T cell epitopes

	Peptide	Position	Amino acid sequence	$CD4^+/CD8^+$ T cell response	Number of participants who responded
Spike ($n=18$)	S-34[a]	166–180	CTFEYVSQPFLMDLE	4/8	10
	S-39	191–205	EFVFKNIDGYFKIYS	NA	1
	S-42	206–230	KHTPI**NLVRDLPQGF**	NA	1
	S-43	211–225	**NLVRDLPQGF**SALEP	NA	1
	S-71	351–365	YAWNRKRISNCVADY	4	1
	S-77	381–395	GVSPTKLNDLCFTNV	4	1
	S-90	446–460	GGNYN**YLYRLFRKSN**	NA	1
	S-91	451–465	**YLYRLFRKSN**LKPFE	NA	1
	S-103	506–520	VVLSFELLHAPATVC	4	1
	S-106	526–540	GPKKSTNLVKNKCVN	8	1
	S-145	721–735	SVTTEILPVSMTKTS	NA	1
	S-150	746–760	STECS**NLLLQYGSFC**	NA	1
	S-151[a]	751–765	**NLLLQYGSFC**TQLNR	4	8
	S-161	801–815	NFSQILPDPSKPSKR	4	2
	S-174[a]	866–880	TDEMIAQYTSALLAG	4	6
	S-235	1,171–1,185	GINASVVNIQKEIDR	NA	1
	S-240	1,196–1,210	LIDLQELGKYEQYI	NA	1
	S-242	1,206–1,220	YEQYIKWPWYIWLGF	NA	1
NP ($n=10$)	NP-1	1–17	MSDNGPQ**NQRNAPRITF**	8	3
	NP-2	8–25	**NQRNAPRITF**GGPSDSTG	8	3
	NP-12	82–95	DQIGYYRRATRRIR	NA	1
	NP-15	101–113	MKD**LSPRWYFYYL**	NA	1
	NP-16[a]	104–121	**LSPRWYFYYL**GTGPEAGL	4/8	12
	NP-46	313–330	AFFGMSRI**GMEVTPSGTW**	NA	1
	NP-47	321–338	**GMEVTPSGTWLTYTGAIK**	NA	1
	NP-48	329–346	**TWLTYTGAIK**LDDKDPNF	4	2
	NP-50	344–361	PNFKDQVI**LLNKHIDAYK**	4	1
	NP-51	352–369	**LLNKHIDAYK**TFPPTEPK	8	3
	M19	133–150	LLESELVI**GAVILRGHLR**	NA	3
M ($n=6$)	M-20[a]	141–158	**GAVILRGHLRIAGHHLGR**	4	11
	M-21	149–166	**LRIAGHHLGR**CDIKDLPK	NA	3
	M-23	165–181	PKEITVA**TSRTLSYYKL**	NA	3
	M-24[a]	172–188	**TSRTLSYYKL**GASQRVA	4	16
	M-28	201–218	IGNYKLNTDHSSSSDNIA	NA	1
ORFs ($n=7$)	ORF3a-20	145–160	YFLCWHTNCYDYCIPY	NA	1
	ORF3a-27	198–215	KDCVVLHS**YFTSDYYQLY**	NA	3
	ORF3a-28	206–225	**YFTSDYYQLY**STQLSTDTGV	8	4
	ORF3a-30	224–243	GVEHVTFFIYNKIVDEPEEH	NA	1
	ORF7a-2	9–25	LITLATCELYHYQECVR	NA	3
	ORF7a-7	46–63	FHPLADNKFALTCFSTQF	NA	1
	ORF7a-10	69–86	DGVKHVYQLRARSVSPKL	4	1

Overlaps of two adjacent peptides recognized by the same participants are shown in bold. [a]Immunodominant peptides. NA, not available.

sensitivities for the different epitopes, it was not possible to make a detailed analysis comparing mild and severe cases. However, the groundwork, including epitope identification, was laid for future studies that can address this important issue.

Multiple strong dominant T cell responses were seen in study participants that were specific for the M and NP proteins. Dominant epitope regions within NP (NP-16) were detected in 35% of study participants, and dominant epitope regions within matrix (M-20 and M-24) were detected in 32 and 47%, respectively. In addition, a higher proportion of multi-cytokine-producing M/NP-specific T cells compared with spike-specific $CD8^+$ T cells were observed in individuals who had recovered from mild disease. A similar trend was also observed in severe cases, although this was not significant, possibly due to fewer cases. These data strongly suggest that NP

Table 2 | Location, sequence and HLA restriction of six identified SARS-CoV2 CD8 optimum epitopes

Protein	Position	Epitope sequence	HLA restriction
NP	9–17	QRNAPRITF	B*2705
	105–113	SPRWYFYYL	B*0702
	322–331	MEVTPSGTWL	B*4001
	362–370	KTFPPTEPK	A*0301
	362–370	KTFPPTEPK	A*1101
ORF3a	207–215	FTSDYYQLY	A*0101

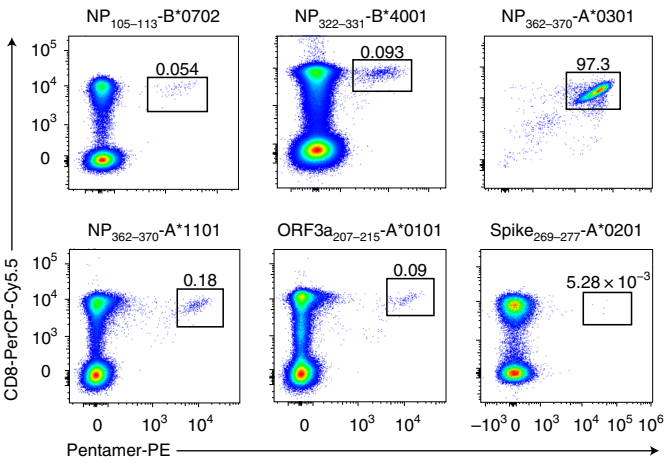

Fig. 6 | Defined SARS-CoV-2-specific CD8 epitopes. Examples of peptide–MHC class I pentamer staining ex vivo, with PBMCs (HLA-B*0702, -B*4001, -A*1101, -A*0101 and -A*0301) or with cultured cell lines (HLA-A*0301). Eleven donors were tested with positive pentamer staining.

and M have the potential for inclusion within future vaccines so as to stimulate strong effector T cell responses. Furthermore, T cells responding to these antigens may be more cross-reactive[18].

IFN-γ-producing SARS-CoV-2-specific T cell responses were not observed in 16 healthy unexposed volunteers, in contrast with recently published reports by Grifoni et al.[17] and Braun et al.[25], both of which used peptide-stimulated activation-induced marker (AIM) assays. In contrast, in a recent immunogenicity study of a recombinant adenovirus type-5-vectored COVID-19 vaccine human phase I trial in 108 volunteers without pre-exposure to COVID-19, spike-specific T cell responses, measured IFN-γ ELISpots and ICS assays were not found before vaccination[6]. These differences could result from differences in the sensitivity of the detection methods.

AIM versus IFN-γ production assays. IFN-γ ELISpot and ICS are well-established methods for evaluating antigen-specific T cells, used in different virus infections and vaccine studies, that have direct functional relevance[24,26–28]. The AIM assay is a more recently developed assay, capable of detecting early-responding T cells, that is independent of cytokine production. Both methods are valid but differ in sensitivity and possible functional relevance. However, it is also possible that different circulating coronaviruses have been previously present in the different geographical populations studied, giving cross-reactive responses in some regions but not others, as suggested by Le Bert et al.[18]. These T cell cross-reacting viruses could include not only SARS-CoV-1 and human common cold coronaviruses, but also other unknown coronaviruses of animal origin. It is also known that very sensitive assays can detect not only

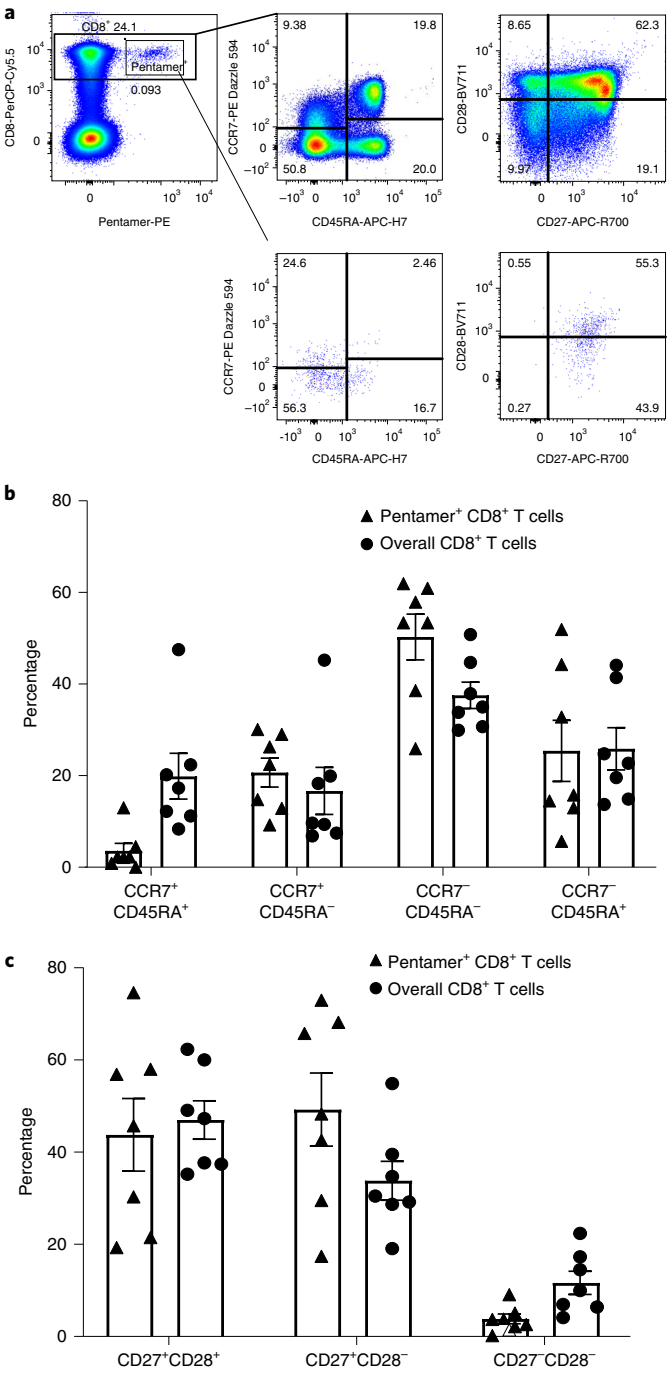

Fig. 7 | Memory phenotype and differentiation status of SARS-CoV-2-specific CD8⁺ T cells. PBMCs were isolated and stained with peptide–MHC class I pentameric complexes and markers of T cell memory and differentiation. **a**, Representative fluorescence-activated cell sorting plots of gating for different cell subsets. **b**,**c**, Expression of memory markers (CCR7 and CD45RA) (**b**) and differentiation markers (CD27 and CD28) (**c**) on CD8⁺ pentamer⁺ T cells. $n = 7$ donors. Data are presented as means ± s.e.m.

pre-existing naive antigen-specific CD4⁺ T cells but also memory CD4⁺ T cells. The latter are potentially primed by other microbes that cross-react with viruses as diverse as CMV, human immunodeficiency virus type 1 and Ebola virus in most unexposed humans[29,30]. Therefore, similar findings with SARS-CoV-2 peptides do not necessarily mean the T cells were primed by previous infecting coronaviruses. Indeed, the implications of pre-existing cross-reactivity

to seasonal coronavirus and other viruses for COVID-19 immunity merit further detailed investigation, as highlighted by Sette and Crotty[31] .

This study focuses on T cell responses in PBMCs. There remains a lack of understanding of memory T cells at the site of infection, which probably provide the most potent protection, as observed in influenza virus infection[32]. It is possible that the hierarchy of immunodominant circulating blood memory T cell pools may not exactly reflect that of memory T cells in the lungs[17,33,34]. Therefore, understanding the features of tissue-resident memory T cells and their association with disease severity will be critical and also merits further investigation.

Taken together, this study has demonstrated strong and broad SARS-CoV-2-specific CD4$^+$ and CD8$^+$ T cell responses in the majority of humans who had recovered from COVID-19. The immunodominant epitope regions and peptides containing T cell epitopes identified in this study will provide critical tools with which to study the contribution of SARS-CoV-19-specific T cells in protection and immune pathology. The identification of non-spike dominant CD8$^+$ T cell epitopes suggests the potential importance of including non-spike proteins such as NP, M and ORFs in future vaccine designs.

Online content

Any methods, additional references, Nature Research reporting summaries, source data, extended data, supplementary information, acknowledgements, peer review information; details of author contributions and competing interests; and statements of data and code availability are available at https://doi.org/10.1038/s41590-020-0782-6.

Received: 2 June 2020; Accepted: 11 August 2020;
Published online: 04 September 2020

References

1. Fehr, A. R. & Perlman, S. in *Coronaviruses. Methods in Molecular Biology* Vol. 1282 (eds Maier H., Bickerton E., Britton P.) 1–23 (Humana Press, 2015).
2. Perlman, S. & Netland, J. Coronaviruses post-SARS: update on replication and pathogenesis. *Nat. Rev. Microbiol.* **7**, 439–450 (2009).
3. Xu, Z. et al. Pathological findings of COVID-19 associated with acute respiratory distress syndrome. *Lancet Respir. Med.* **8**, 420–422 (2020).
4. Guan, W. J. et al. Clinical characteristics of coronavirus disease 2019 in China. *N. Engl. J. Med.* **382**, 1708–1720 (2020).
5. Yu, J. et al. DNA vaccine protection against SARS-CoV-2 in rhesus macaques. *Science* **369**, 806–811 (2020).
6. Zhu, F. C. et al. Safety, tolerability, and immunogenicity of a recombinant adenovirus type-5 vectored COVID-19 vaccine: a dose-escalation, open-label, non-randomised, first-in-human trial. *Lancet* **395**, 1845–1854 (2020).
7. van Doremalen, N. et al. ChAdOx1 nCoV-19 vaccination prevents SARS-CoV-2 pneumonia in rhesus macaques. *Nature* https://doi.org/10.1038/s41586-020-2608-y (2020).
8. Folegatti, P. M. et al. Safety and immunogenicity of the ChAdOx1 nCoV-19 vaccine against SARS-CoV-2: a preliminary report of a phase 1/2, single-blind, randomised controlled trial. *Lancet* **396**, P467–P478 (2020).
9. St John, A. L. & Rathore, A. P. S. Adaptive immune responses to primary and secondary dengue virus infections. *Nat. Rev. Immunol.* **19**, 218–230 (2019).
10. Huang, C. et al. Clinical features of patients infected with 2019 novel coronavirus in Wuhan, China. *Lancet* **395**, 497–506 (2020).
11. Liao, M. et al. Single-cell landscape of bronchoalveolar immune cells in patients with COVID-19. *Nat. Med.* **26**, 842–844 (2020).
12. Chen, Y. et al. The novel severe acute respiratory syndrome coronavirus 2 (SARS-CoV-2) directly decimates human spleens and lymph nodes. Preprint at *medRxiv* https://doi.org/10.1101/2020.03.27.20045427 (2020).
13. Diao, B. et al. Reduction and functional exhaustion of T cells in patients with coronavirus disease 2019 (COVID-19). *Front. Immunol.* **11**, 827 (2020).
14. Pereira, B. I. et al. Sestrins induce natural killer function in senescent-like CD8$^+$ T cells. *Nat. Immunol.* **21**, 684–694 (2020).
15. Ni, L. et al. Detection of SARS-CoV-2-specific humoral and cellular immunity in COVID-19 convalescent individuals. *Immunity* **52**, 971–977.e3 (2020).
16. Hayward, A. C. et al. Natural T cell-mediated protection against seasonal and pandemic influenza. Results of the Flu Watch cohort study. *Am. J. Respir. Crit. Care Med.* **191**, 1422–1431 (2015).
17. Grifoni, A. et al. Targets of T cell responses to SARS-CoV-2 coronavirus in humans with COVID-19 disease and unexposed individuals. *Cell* **181**, 1489–1501.e15 (2020).
18. Le Bert, N. et al. SARS-CoV-2-specific T cell immunity in cases of COVID-19 and SARS, and uninfected controls. *Nature* https://doi.org/10.1038/s41586-020-2550-z (2020).
19. Wilkinson, T. M. et al. Preexisting influenza-specific CD4$^+$ T cells correlate with disease protection against influenza challenge in humans. *Nat. Med.* **18**, 274–280 (2012).
20. Ahmed, S. F., Quadeer, A. A. & McKay, M. R.Preliminary identification of potential vaccine targets for the COVID-19 coronavirus (SARS-CoV-2) based on SARS-CoV immunological studies. *Viruses* **12**, 254 (2020).
21. Ogg, G. S. et al. Four novel cytotoxic T-lymphocyte epitopes in the highly conserved major homology region of HIV-1 Gag, restricted through B*4402, B*1801, A*2601, B*70 (B*1509). *AIDS* **12**, 1561–1563 (1998).
22. Shomuradova, A. S. et al. SARS-CoV-2 epitopes are recognized by a public and diverse repertoire of human T-cell receptors. Preprint at *medRxiv* https://doi.org/10.1101/2020.05.20.20107813 (2020).
23. Sekine, T. et al. Robust T cell immunity in convalescent individuals with asymptomatic or mild COVID-19. *Cell* https://doi.org/10.1016/j.cell.2020.08.017 (2020).
24. Lee, L. Y. et al. Memory T cells established by seasonal human influenza A infection cross-react with avian influenza A (H5N1) in healthy individuals. *J. Clin. Invest.* **118**, 3478–3490 (2008).
25. Braun, J. et al. SARS-CoV-2-reactive T cells in healthy donors and patients with COVID-19. *Nature* https://doi.org/10.1038/s41586-020-2598-9 (2020).
26. Li, C. K. et al. T cell responses to whole SARS coronavirus in humans. *J. Immunol.* **181**, 5490–5500 (2008).
27. Powell, T. J. et al. Identification of H5N1-specific T-cell responses in a high-risk cohort in Vietnam indicates the existence of potential asymptomatic infections. *J. Infect. Dis.* **205**, 20–27 (2012).
28. Dong, T. et al. Extensive HLA-driven viral diversity following a narrow-source HIV-1 outbreak in rural China. *Blood* **118**, 98–106 (2011).
29. Su, L. F. & Davis, M. M. Antiviral memory phenotype T cells in unexposed adults. *Immunol. Rev.* **255**, 95–109 (2013).
30. Campion, S. L. et al. Proteome-wide analysis of HIV-specific naive and memory CD4$^+$ T cells in unexposed blood donors. *J. Exp. Med.* **211**, 1273–1280 (2014).
31. Sette, A. & Crotty, S.Pre-existing immunity to SARS-CoV-2: the knowns and unknowns. *Nat. Rev. Immunol.* **20**, 457–458 (2020).
32. Pizzolla, A. et al. Resident memory CD8$^+$ T cells in the upper respiratory tract prevent pulmonary influenza virus infection. *Sci. Immunol.* **2**, eaam6970 (2017).
33. Turner, D. L. et al. Lung niches for the generation and maintenance of tissue-resident memory T cells. *Mucosal Immunol.* **7**, 501–510 (2014).
34. Yoshizawa, A. et al. TCR–pMHC encounter differentially regulates transcriptomes of tissue-resident CD8 T cells. *Eur. J. Immunol.* **48**, 128–150 (2018).

[1]MRC Human Immunology Unit, MRC Weatherall Institute of Molecular Medicine, Radcliffe Department of Medicine, University of Oxford, Oxford, UK. [2]Chinese Academy of Medical Sciences (CAMS) Oxford Institute (COI), University of Oxford, Oxford, UK. [3]Wellcome Centre for Human Genetics, University of Oxford, Oxford, UK. [4]Nuffield Department of Medicine, University of Oxford, Oxford, UK. [5]Oxford University Hospitals NHS Foundation Trust, Oxford, UK. [6]Beijing You'an Hospital, Capital Medical University, Beijing, China. [7]CAMS Key Laboratory of Tumor Immunology and Radiation Therapy, Xinjiang Tumor Hospital, Xinjiang Medical University, Xinjiang, China. [8]Sequencing and Flow Cytometry Facility, Weatherall Institute of Molecular Medicine, University of Oxford, Oxford, UK. [9]Diamond Light Source, Didcot, UK. [10]York Structural Biology Laboratory, Department of Chemistry, University of York, York, UK. [11]Tropical and Infectious Diseases Unit, Liverpool University Hospitals NHS Foundation Trust, Liverpool, UK. [12]NIHR Health Protection Research Unit in Emerging and Zoonotic Infections, Institute of Infection, Veterinary and Ecological Sciences, University of Liverpool, Liverpool, UK.

[13]Oxford Vaccine Group, Department of Paediatrics, University of Oxford, Oxford, UK. [14]NIHR Oxford Biomedical Research Centre, Centre for Clinical Vaccinology and Tropical Medicine, University of Oxford, Oxford, UK. [15]The Florey Institute for Host–Pathogen Interactions, Department of Infection, Immunity and Cardiovascular Disease, University of Sheffield, Sheffield, UK. [16]ProImmune, Oxford, UK. [17]Respiratory Medicine, Institute in The Park, Alder Hey Children's Hospital, Liverpool, UK. [18]Anaesthesia, Critical Care and Pain Medicine Division of Health Sciences, University of Edinburgh, Edinburgh, UK. [19]National Heart and Lung Institute, Faculty of Medicine, Imperial College London, London, UK. [20]NIHR Oxford Biomedical Research Centre, Oxford, UK. [21]Worthing Hospital, Worthing, UK. [22]Dengue Hemorrhagic Fever Research Unit, Office for Research and Development, Faculty of Medicine, Siriraj Hospital, Mahidol University, Bangkok, Thailand. [23]These authors contributed equally: Yanchun Peng, Alexander J. Mentzer, Guihai Liu, Xuan Yao, Zixi Yin, Danning Dong, Wanwisa Dejnirattisai. [24]These authors jointly supervised this work: Graham Ogg, Tao Dong. *A full list of members appears in the Supplementary Information. ✉e-mail: tao.dong@imm.ox.ac.uk

Oxford Immunology Network Covid-19 Response T cell Consortium

Eleanor Barnes[4,5,20], Danning Dong[2,4,7,23], Tao Dong[1,2,4,24], Susanna Dunachie[4,5], John Frater[4,5], Philip Goulder[4,5], Georgina Kerr[4], Paul Klenerman[4,5,20], Guihai Liu[2,4,6,23], Andrew McMichael[2,4], Giorgio Napolitani[1], Graham Ogg[1,2,5,20,24], Yanchun Peng[1,2,23], Mariolina Salio[1], Xuan Yao[1,2,4] and Zixi Yin[1,2,23]

ISARIC4C Investigators

J. Kenneth Baillie[18], Paul Klenerman[4,5,20], Alexander J. Mentzer[3,4,5,23], Shona C. Moore[12], Peter J. M. Openshaw[19], Malcolm G. Semple[12,17], David I. Stuart[2,3,4,9] and Lance Turtle[11,12]

Methods

Ethics. Patients were recruited from the John Radcliffe Hospital in Oxford, United Kingdom, between March and May 2020 by the identification of patients hospitalized during the SARS-COV-2 pandemic and recruited into the Sepsis Immunomics and International Severe Acute Respiratory and Emerging Infection Consortium World Health Organization Clinical Characterisation Protocol UK (IRAS260007 and IRAS126600). Patients were sampled at least 28 d from the start of their symptoms. Unexposed healthy adult donor samples were used from unrelated studies undertaken between 2017 and early 2019. Written informed consent was obtained from all patients. Ethical approval was given by the South Central–Oxford C Research Ethics Committee in England (reference: 13/SC/0149), Scotland A Research Ethics Committee (reference: 20/SS/0028) and World Health Organization Ethics Review Committee (RPC571 and RPC572l; 25 April 2013).

Clinical definitions. All patients were confirmed to have a test positive for SARS-CoV-2 using PCR with reverse transcription from an upper respiratory tract (nose and throat) swab tested at an accredited laboratory. The degree of severity was identified as mild, severe or critical infection, according to recommendations from the World Health Organization. Patients were classified as having mild symptoms if they did not require oxygen (that is, their oxygen saturation was greater than 93% on ambient air) or if their symptoms were managed at home. A large proportion of our mild cases were admitted to hospital for public health reasons during the early phase of the pandemic even though they had no medical reason to be admitted to hospital. Severe infection was defined as one of the following conditions in a patient confirmed as having COVID-19: respiratory distress with a respiratory rate of >30 breaths per minute; blood oxygen saturation of <93%; or arterial oxygen partial pressure/FiO_2 < 300 mmHg. Critical infection was defined as: respiratory failure requiring mechanical ventilation or shock; or other organ failures requiring admission to an intensive care unit. Since the severe classification could potentially include individuals spanning a wide spectrum of disease severity, ranging from patients receiving oxygen through a nasal cannula through to those receiving non-invasive ventilation, we also calculated the SaO_2/FiO_2 ratio at the height of patient illness as a quantitative marker of lung damage. This was calculated by dividing the oxygen saturation (as determined using a bedside pulse oximeter) by the fraction of inspired oxygen (21% for ambient air; 24% for nasal cannulae; 28% for simple face masks; 28, 35, 40 or 60% for Venturi face masks; or precise measurements for non-invasive or invasive ventilation settings). Patients not requiring oxygen who had oxygen saturations (if measured) greater than 93% on ambient air or managed at home were classified as having mild disease. Viral swab Ct values were not available for all patients. In addition, we standardized all of our analyses to the days since symptom onset.

Synthetic peptides. A total of 423 15- to 18-mer peptides overlapping by ten amino acid residues and spanning the full proteome of SARS-CoV-2 except ORF1 (Supplementary Table 1) were designed using the software PeptGen (http://www.hiv.lanl.gov/content/sequence/PEPTGEN/peptgen.html) and synthesized (purity: >75%; ProImmune).

A total of 27 previously defined SARS epitopes[20] were also synthesized (Supplementary Table 2). Pools of CMV, Epstein–Barr virus and influenza virus-specific epitope peptides and the human immunodeficiency virus Gag protein were also used as positive and negative controls.

Two-dimensional peptide matrix system. The overlapping peptides spanning SARS-CoV-2 were assigned to a two-dimensional matrix system in which each peptide was represented in two different peptide pools. Each peptide pool contained no more than 16 individual peptides. The first dimension of the peptide matrix system was designed so that peptides from different source proteins were separated into different pools. (Supplementary Table 1).

Ex vivo ELISpot assay. IFN-γ ELISpot assays were performed using either freshly isolated or cryopreserved PBMCs, as described previously. No significant difference was observed between responses generated by fresh and cryopreserved PBMCs, as described previously[24,35].

Overlapping peptides were pooled and then added to 200,000 PBMCs per test at a final concentration of 2 μg ml^{-1} for 16–18 h. The positive responses were confirmed by repeat ELISpot assays. To quantify antigen-specific responses, mean spots of the control wells were subtracted from the positive wells, and the results were expressed as spot-forming units (s.f.u.) per 10^6 PBMCs. Responses were considered positive if the results were at least three times the mean of the negative control wells and >25 s.f.u. per 10^6 PBMCs. If negative control wells had >30 s.f.u. per 10^6 PBMCs or positive control wells (phytohemagglutinin stimulation) were negative, the results were excluded from further analysis.

Determination of plasma binding to trimeric spike, RBD and NP by enzyme-linked immunosorbent assay. MaxiSorp immunoplates (442404; NUNC) were coated with 0.125 μg StrepMAB-Classic (2-1507-001; IBA), blocked with 2% skimmed milk in phosphate-buffered saline (PBS) for 1 h and then incubated with 50 μl of 5 μg ml^{-1} soluble trimeric spike and 2 μg ml^{-1} of 2% skimmed milk in PBS. After 1 h, 50 μl of serial twofold dilutions of plasma, from 1:50 to 1:51,200 in PBS containing 2% skimmed milk, were added followed by alkaline-phosphatase-conjugated anti-human IgG (A9544; Sigma–Aldrich) at 1:10,000 dilution. The reaction was developed by the addition of *para*-nitrophenyl phosphate substrate and stopped with NaOH. The absorbance was measured at 405 nm. EPTs were defined as reciprocal plasma dilutions that corresponded to two times the average optical density values obtained with mock. To determine EPTs to RBD and NP, immunoplates were coated with 0.125 μg Tetra-His antibody (34670; Qiagen) followed by 2 and 5 μg ml^{-1} of soluble RBD and NP, respectively.

ICS. ICS was performed as described previously[36,37]. Briefly, overnight-rested PBMCs were stimulated with pooled or individual peptides at a final concentration of 10 μg ml^{-1} for 1 h in the presence of 2 μg ml^{-1} monoclonal antibodies CD28 and CD49d, and then for an additional 5 h with GolgiPlug, GolgiStop, and surface stained with PE-anti-CD107a. Dead cells were labeled using LIVE/DEAD Fixable Aqua dye from Invitrogen. Surface markers, including BUV395-anti-CD3, BUV737-anti-CD4, PerCP-Cy5.5-anti-CD8, BV510-anti-CD14, BV510-anti-CD16 and BV510-anti-CD19 (BioLegend) were stained. Cells were then washed, fixed with Cytofix/Cytoperm and stained with PE-Cy7-anti-IFNγ (eBioscience), APC-anti-TNFα (eBioscience) or BV421-anti-IL-2 (BioLegend). Negative controls without peptide stimulation were run for each sample. All reagents were from BD Biosciences unless otherwise stated. All samples were acquired on a BD LSRFortessa (BD Biosciences) flow cytometer and analyzed using FlowJo version 10 software. Peptide-pool-reactive $CD4^+$ or $CD8^+$ T cells with a frequency lower than 0.05% of $CD4^+$ or $CD8^+$ T cells, respectively, were excluded from analysis. Cytokine responses were background subtracted individually before further analysis. To determine the frequency of different response patterns based on all possible combinations, Boolean gates were created using IFN-γ, TNF-α and IL-2. Cytokine responses were background subtracted individually before further analysis.

Pentamer phenotyping. Cryopreserved PBMCs were thawed, as described above. A total of 1×10^6 live PBMCs were labeled with peptide–MHC class I Pentamer-PE (ProImmune) and incubated for 15 min at 37 °C. Dead cells were first labeled with LIVE/DEAD Fixable Aqua dye (Invitrogen) and then with the surface markers CD3-BUV395, CD8-PerCP.Cy5.5, CD14-BV510, CD16-BV510, CD19-BV510, CD28-BV711, CD27-APC-R700, CD45RA-APC-H7 and CCR7-PE-Dazzel 594 (BioLegend). All reagents were from BD Biosciences unless otherwise stated. All samples were acquired on a BD LSRFortessa (BD Biosciences) flow cytometer and analyzed using FlowJo version 10 software.

Generation of short-term T cell lines. Short-term SARS-CoV-2-specific T cell lines were established as previously described[35]. Briefly, 3×10^6 to 5×10^6 PBMCs were pulsed as a pellet for 1 h at 37 °C with 10 μM of peptides containing T cell epitope regions and cultured in R10 at 2×10^6 cells per well in a 24-well Costar plate. IL-2 was added to a final concentration of 100 U ml^{-1} on day 3 and cultured for further 10–14 d.

Statistical analysis. Statistical analysis was performed with IBM SPSS Statistics 25 and the figures were made with GraphPad Prism 8. Chi-squared tests were used to compare ratio differences between two groups. After testing for normality using the Kolmogorov–Smirnov test, the independent-samples *t*-test or Mann–Whitney *U*-test was employed to compare variables between two groups. Correlations were performed via Spearman's rank correlation. Statistical significance was set at $^*P < 0.05$, $^{**}P < 0.01$, $^{***}P < 0.001$ and $^{****}P < 0.0001$. All of the tests were two tailed.

Reporting Summary. Further information on research design is available in the Nature Research Reporting Summary linked to this article.

Data availability

Data relating to the findings of this study are available from the corresponding author upon request. Source data are provided with this paper.

References

35. Peng, Y. et al. Boosted influenza-specific T cell responses after H5N1 pandemic live attenuated influenza virus vaccination. *Front. Immunol.* **6**, 287 (2015).
36. Lillie, P. J. et al. Preliminary assessment of the efficacy of a T-cell-based influenza vaccine, MVA-NP+M1, in humans. *Clin. Infect. Dis.* **55**, 19–25 (2012).
37. De Silva, T. I. et al. Correlates of T-cell-mediated viral control and phenotype of $CD8^+$ T cells in HIV-2, a naturally contained human retroviral infection. *Blood* **121**, 4330–4339 (2013).

Acknowledgements

We are grateful to all of the participants for donating their samples and data for these analyses, and to the research teams involved in the consenting, recruitment and sampling of these participants. We acknowledge the support of the Oxford Immunology Network COVID-19 Response T Cell Consortium (Supplementary Table 4) and ISARIC4C

Investigators (Supplementary Table 5). This work is supported by the UK Medical Research Council (to T.D., G.O., Y.P., M.S., G.N. and Y.-L.C.); Chinese Academy of Medical Sciences (CAMS) Innovation Fund for Medical Sciences (CIFMS), China (grant number 2018-I2M-2-002 to T.D., Y.P., X.Y., G.L., D.D., D.I.S., J.M. and G.R.S.); National Institutes of Health, National Key R&D Program of China (2020YFE0202400 to T.D., Y. Zhang and R.J.); China Scholarship Council (Z.Y., G.L. and C.L.); National Institute for Health Research (NIHR) (award CO-CIN-01 to M.G.S.); Medical Research Council (grant MC_PC_19059 to M.G.S.); Wellcome Trust and Department for International Development (215091/Z/18/Z to M.G.S.); and the Bill and Melinda Gates Foundation (OPP1209135 to M.G.S.). The study is also funded by the NIHR Oxford Biomedical Research Centre (to L.-P.H., G.O., P.K., E.B. and G.R.S.), Senior Investigator Award (to G.O.), Clinical Research Network (to G.O.), Schmidt Futures (G.R.S.), Health Protection Research Unit in Respiratory Infections (NIHR200927/WHRG_P82523 to P.J.M.O.), NIHR Senior Investigator Award (NIHR201385/WHRR P84026 to P.J.M.O.), Imperial College Biomedical Research Centre (IS-BRC-1215-20013 to P.J.M.O.) and National Institute of Allergy and Infectious Diseases (Consortium for HIV/AIDS Vaccine Development UM1 AI 144371 to P.B. and A.M. and R01 AI 118549 to P.B.). L.T., P.K. and P. Simmonds are supported by the NIHR Health Protection Research Unit (HPRU) in Emerging and Zoonotic Infections (NIHR200907) at the University of Liverpool in partnership with Public Health England (PHE), in collaboration with the Liverpool School of Tropical Medicine and University of Oxford. L.T. is based at the University of Liverpool. P.K. and P. Simmonds are based at the University of Oxford. L.T., T.d.S. and A.A.A. are supported by the Wellcome Trust (grant numbers 205228/Z/16/Z to L.T., 110058/Z/15/Z to T.d.S. and 206377 to A.A.A.). G.R.S. is supported as a Wellcome Trust Senior Investigator (grant 095541/A/11/Z). P.B. and A.M. are Jenner Institute investigators. This work uses data provided by patients and collected by the NHS as part of their care, and supports the Data Saves Lives initiative. The views expressed are those of the authors and not necessarily those of the Department of Health and Social Care, DID, NIHR, MRC, Wellcome Trust or PHE.

Author contributions

T.D. and G.O. conceptualized the project. T.D. and Y.P. designed and supervised the T cell experiments. J.M. and G.R.S. designed the antibody experiments. Y.P., G.L., X.Y., Z.Y. and D.D. performed all of the T cell experiments. W.D., J.M., P. Supasa, C.L., C.L.-C., J.S.-c., Y. Zhao, D.I.S., G.C.P., J.M.G., A.A.A., O.W.B., D.E.D.P.H., B.W. and D.-S.K. performed the spike, RBD and NP EPT experiments. T.R. performed the HLA typing. J.C.K., A.J.M., T.L., R.L., P.K., T.d.S., M.G.S., C.P.C., S.C.M., J.K.B. and P.J.M.O. established the clinical cohorts and collected the clinical samples and data. K.S., P.T., P.Z., C.D., J.R., P. Simmonds, P. Sopp, D.W., U.R., Y.-L.C., W.P., P.B., J.W.F., N.F.S., M.A.A., S.D., M.S., G.N., E.B., G.K., P.G., Y. Zhang, R.J. and L.-P.H. provided the critical reagents and technical assistance. Y.P., G.L., X.Y., Z.Y., D.D., W.D., P.Z. and J.M. analyzed the data. T.D. wrote the original draft. G.O., J.C.K., A.M., A.J.M., P.B., P.K., P.J.M.O., L.T., G.R.S., R.J.C., P.S., M.G.S., B.M.K. and C.P.C. reviewed and edited the manuscript and figures.

Competing interests

The authors declare no competing interests.

Additional information

Supplementary information is available for this paper at https://doi.org/10.1038/s41590-020-0782-6.

Correspondence and requests for materials should be addressed to T.D.

Peer review information J. D. K. Wilson was the primary editor on this article and managed its editorial process and peer review in collaboration with the rest of the editorial team.

Reprints and permissions information is available at www.nature.com/reprints.

nature research

Corresponding author(s): Tao Dong

Last updated by author(s): Aug 5, 2020

Reporting Summary

Nature Research wishes to improve the reproducibility of the work that we publish. This form provides structure for consistency and transparency in reporting. For further information on Nature Research policies, see our Editorial Policies and the Editorial Policy Checklist.

Statistics

For all statistical analyses, confirm that the following items are present in the figure legend, table legend, main text, or Methods section.

n/a	Confirmed	
☐	☒	The exact sample size (*n*) for each experimental group/condition, given as a discrete number and unit of measurement
☐	☒	A statement on whether measurements were taken from distinct samples or whether the same sample was measured repeatedly
☐	☒	The statistical test(s) used AND whether they are one- or two-sided *Only common tests should be described solely by name; describe more complex techniques in the Methods section.*
☐	☒	A description of all covariates tested
☐	☒	A description of any assumptions or corrections, such as tests of normality and adjustment for multiple comparisons
☐	☒	A full description of the statistical parameters including central tendency (e.g. means) or other basic estimates (e.g. regression coefficient) AND variation (e.g. standard deviation) or associated estimates of uncertainty (e.g. confidence intervals)
☐	☒	For null hypothesis testing, the test statistic (e.g. *F*, *t*, *r*) with confidence intervals, effect sizes, degrees of freedom and *P* value noted *Give P values as exact values whenever suitable.*
☒	☐	For Bayesian analysis, information on the choice of priors and Markov chain Monte Carlo settings
☒	☐	For hierarchical and complex designs, identification of the appropriate level for tests and full reporting of outcomes
☒	☐	Estimates of effect sizes (e.g. Cohen's *d*, Pearson's *r*), indicating how they were calculated

Our web collection on statistics for biologists contains articles on many of the points above.

Software and code

Policy information about availability of computer code

Data collection	ELISpot data were collected with AID ELISpot 7.0 and flow cytometry data were collected by BD FACSDiva V9.0
Data analysis	Flow cytometry data were analyzed with FlowJoTM v.10.5.3 software for Mac. Prism version 8.2.1 for Mac OS and IBM SPSS Statistic 25 were used for statistical analysis

For manuscripts utilizing custom algorithms or software that are central to the research but not yet described in published literature, software must be made available to editors and reviewers. We strongly encourage code deposition in a community repository (e.g. GitHub). See the Nature Research guidelines for submitting code & software for further information.

Data

Policy information about availability of data

All manuscripts must include a data availability statement. This statement should provide the following information, where applicable:

- Accession codes, unique identifiers, or web links for publicly available datasets
- A list of figures that have associated raw data
- A description of any restrictions on data availability

The raw data from all the main figures and supplementary figures are available upon request.

Field-specific reporting

Please select the one below that is the best fit for your research. If you are not sure, read the appropriate sections before making your selection.

☒ Life sciences ☐ Behavioural & social sciences ☐ Ecological, evolutionary & environmental sciences

For a reference copy of the document with all sections, see nature.com/documents/nr-reporting-summary-flat.pdf

Life sciences study design

All studies must disclose on these points even when the disclosure is negative.

Sample size	42 subjects recovered from COVID-19 and 19 unexposed healthy control samples. This was a discovery project for identifying new epitopes in an unpublished UK population, and so predictive sample size calculations were challenging. Samples sizes were based on maximal available samples sets where detailed clinical and serological data were also available, and aligned well with our previously published data in other settings, including influenza and HIV (Lee et al, JCI 2008; Zhang et al, NC 2013; Zhao et al, AJCCM 2012)
Data exclusions	For ELISPOT assays, If negative control wells had >30 SFU/106 PBMCs or positive control wells (PHA stimulation) were negative, the results were excluded from further analysis.
Replication	Samples analyzed in this study were from participants of a cohort study and samples were analyzed on individual study participants. Experiments did not include replicates as all participants and data points are unique. Some of the experiments used technical and/or biological replicates, and all attempts were successful. Some results were confirmed by different methods.
Randomization	Randomization was not appropriate for this study of immune responses in COVID-19 convalescent individuals, with no associated therapeutic intervention
Blinding	Blinding was not appropriate for this study of immune responses in COVID-19 convalescent individuals, with no associated therapeutic intervention

Reporting for specific materials, systems and methods

We require information from authors about some types of materials, experimental systems and methods used in many studies. Here, indicate whether each material, system or method listed is relevant to your study. If you are not sure if a list item applies to your research, read the appropriate section before selecting a response.

Materials & experimental systems

n/a	Involved in the study
☐	☒ Antibodies
☒	☐ Eukaryotic cell lines
☒	☐ Palaeontology and archaeology
☒	☐ Animals and other organisms
☐	☒ Human research participants
☒	☐ Clinical data
☒	☐ Dual use research of concern

Methods

n/a	Involved in the study
☒	☐ ChIP-seq
☐	☒ Flow cytometry
☒	☐ MRI-based neuroimaging

Antibodies

Antibodies used

Antibodies used for ELISA

Marker	Supplier	Cat number	Clone	Lot Number	Dilution
StrepMAB-Classic	IBA	2-1507-001	N/A	1507-0045	2.5ug/ml
ALP-conjugated anti-human IgG	Sigma	A9544	Polyclonal	0000887076	1:10,000
Tetra-His antibody	QIAGEN	34670	N/A	163028277	2.5ug/ml

Antibodies used for flow cytometry

Marker	Fuorophore	Supplier	Cat number	Clonotype	Lot Number	Dilution
CD28/CD49d	NA	BD Bioscience	347690	L392/L25	9315490	1:100
CD14	BV510	BioLegend	301842	M5E2	B265263	1:50
CD16	BV510	BioLegend	302048	3G8	B259404	1:50
CD19	BV510	BioLegend	302242	HIB19	B242298	1:50
CD3	BUV395	BD Bioscience	564001	SK7	9322768	1:33
CD4	BUV737	BD Bioscience	564305	SK3	8276889	1:33
CD8	PerCP-Cy5.5	BD Bioscience	565310	SK1	8284703	1:33
IFNg	PE-Cy7	BD Bioscience	557643	B27	9332967	1:33

TNFa	APC	eBioscience	17-7349-82	MAb11	1973586	1:500
IL-2	BV421	BioLegend	500328	MQ1-17H12	B254112	1:33
CD107a	PE	BD Bioscience	555801	H4A3	8130821	1:20
CD28	BV711	BD Bioscience	563131	CD28.2	57622	1:50
CD27	APC-R700	BD Bioscience	565116	M-T271	9106651	1:33
CCR7	PE/Dazzle 594	BioLegend	353236	G043H7	B280709	1:50
CD45RA	APC-H7	BD Bioscience	560674	HI100	8149697	1:33

Validation

All antibodies used in this study are commercially available. Antibodies used in a specific species or application have been appropriately validated by manufacturers for that application and this information is provided on their website and product information datasheets. All antibodies described here have been further optimized for an appropriate concentration by testing several dilutions.
StrepMAB-Classic https://www.iba-lifesciences.com/details/product/2-1507-001.html
ALP-conjugated anti-human IgG https://www.sigmaaldrich.com/catalog/product/sigma/a9544?lang=en&region=GB
Tetra-His antibody https://www.qiagen.com/gb/products/discovery-and-translational-research/protein-purification/tagged-protein-expression-purification-detection/tetra-his-antibody-bsa-free/#productdetails
anti-CD28/anti-CD49d https://www.bdbiosciences.com/eu/reagents/research/clinical-research---ruo-gmp/purified-antibodies/anti-human-cd28cd49d-purified-l293-l25/p/347690
CD14 https://www.biolegend.com/en-us/products/brilliant-violet-510-anti-human-cd14-antibody-8001
CD16 https://www.biolegend.com/en-us/products/brilliant-violet-510-anti-human-cd16-antibody-8003
CD19 https://www.biolegend.com/en-us/products/brilliant-violet-510-anti-human-cd19-antibody-8004
CD3 https://www.bdbiosciences.com/eu/applications/research/t-cell-immunology/th-1-cells/surface-markers/human/buv395-mouse-anti-human-cd3-sk7-also-known-as-leu-4/p/564001
CD4 https://www.bdbiosciences.com/eu/reagents/research/antibodies-buffers/immunology-reagents/anti-human-antibodies/cell-surface-antigens/buv737-mouse-anti-human-cd4-sk3-also-known-as-leu3a/p/612748
CD8 https://www.bdbiosciences.com/eu/reagents/research/antibodies-buffers/immunology-reagents/anti-non-human-primate-antibodies/cell-surface-antigens/percp-cy55-mouse-anti-human-cd8-sk1/p/565310
IFN-g https://www.bdbiosciences.com/eu/applications/research/t-cell-immunology/th-1-cells/intracellular-markers/cytokines-and-chemokines/human/pe-cy7-mouse-anti-human-ifn--b27/p/557643
TNFa https://www.thermofisher.com/antibody/product/TNF-alpha-Antibody-clone-MAb11-Monoclonal/17-7349-82
IL-2 https://www.biolegend.com/en-us/products/brilliant-violet-421-anti-human-il-2-antibody-7148
CD107a https://www.bdbiosciences.com/eu/applications/research/intracellular-flow/intracellular-antibodies-and-isotype-controls/anti-human-antibodies/pe-mouse-anti-human-cd107a-h4a3/p/555801
CD28 https://www.bdbiosciences.com/eu/applications/research/t-cell-immunology/regulatory-t-cells/surface-markers/human/bv711-mouse-anti-human-cd28-cd282/p/563131
CD27 https://www.bdbiosciences.com/eu/reagents/research/antibodies-buffers/immunology-reagents/anti-human-antibodies/cell-surface-antigens/apc-r700-mouse-anti-human-cd27-m-t271/p/565116
CD45RA https://www.bdbiosciences.com/eu/applications/research/b-cell-research/surface-markers/human/apc-h7-mouse-anti-human-cd45ra-hi100/p/560674
CCR7 https://www.biolegend.com/en-us/products/pe-dazzle-594-anti-human-cd197-ccr7-antibody-9811

Human research participants

Policy information about studies involving human research participants

Population characteristics

42 individuals were recruited following recovery from COVID-19, including 28 mild cases and 14 severe cases. In addition, 15 control individuals sampled in the pre-COVID-19 season were studied in parallel. Supplementary Figure 1 shows the participant characteristics. No significant differences in gender or age were noted between mild and severe groups. The SaO2/FiO2 ratio in severe cases ranged from 4.3 (where 4.5 would be the estimate for an individual with mild disease breathing ambient air) to 1.6 with the patients with critical disease having an estimate of 0.8 (median in severe group 3.8).

Recruitment

Patients were recruited from the John Radcliffe Hospital in Oxford, UK, between March and May 2020 by identification of patients hospitalised during the SARS-COV-2 pandemic and recruited into the Sepsis Immunomics and ISARIC Clinical Characterisation Protocols. Patients were sampled at least 28 days from the start of their symptoms. Unexposed healthy adult donor samples were used from unrelated studies undertaken between 2017-early 2019. Written informed consent was obtained from all patients. The potential bias, such as the timing when samples were taken, the gender and age of the patients, are unlikely to impact the results, as there is no significant difference in the age between two study groups, and no correlation was observed between the T cell response and days post symptoms when samples were taken

Ethics oversight

The samples were collected from patients with confirmed COVID who had consented to participate in either or both of the following studies: The GAinS investigators: application of an integrated immune -omic approach in sepsis (known as the Sepsis Immunomic project IRAS 260007 approved by the South Central - Oxford C Research Ethics Committee in England and the ISARIC/WHO Clinical Characterisation Protocol for Severe Emerging Infections (IRAS126600). Ethical approval was given by the South Central - Oxford C Research Ethics Committee in England (Ref 13/SC/0149), the Scotland A Research Ethics Committee (Ref 20/SS/0028), and the WHO Ethics Review Committee (RPC571 and RPC572, 25 April 2013)

Note that full information on the approval of the study protocol must also be provided in the manuscript.

Flow Cytometry

Plots

Confirm that:

☒ The axis labels state the marker and fluorochrome used (e.g. CD4-FITC).

☒ The axis scales are clearly visible. Include numbers along axes only for bottom left plot of group (a 'group' is an analysis of identical markers).

☒ All plots are contour plots with outliers or pseudocolor plots.

☒ A numerical value for number of cells or percentage (with statistics) is provided.

Methodology

Sample preparation	Cryopreserved PBMCs were thawed and rested overnight in R10 at 37oC. On the second day, for intracellular cytokine staining (ICS), the PBMCs were stimulated with pooled or individual peptides for 1 h in the presence of 2 µg/mL monoclonal antibodies against human CD28 (BD Pharmingen) and CD49d (BD Pharmingen) then for an additional 5h with GolgiPlug (brefeldin A, BD), GolgiStop (monensin, BD) and surface stained with PE-anti-CD107a (BD Biosciences). For Pentamer phenotyping, overnight rested cells were first labeled with Pentamers for 15mins at 37oC. Then a standard FACS staining was carried out. Briefly, dead cells were first labelled with LIVE/DEAD™ Fixable Aqua dye and then followed by surface antibody staining. Subsequently, Cytofix/CytopermTM kit (BD Biosciences) was used for permeabillizing the cells before staining the cells with antibodies against molecules expressed intracellularly. Finally, cells then be fixed with 1X cell fixing buffer.
Instrument	Samples were acquired at BD LSR Fortessa X20
Software	Data were analyzed using FlowJoTM v.10 software for Mac.
Cell population abundance	There is no sorting involved in this study.
Gating strategy	For all the experiments, cells were first gated on single Lymphocytes by a forward side scatter gate, followed by CD3/ CD4/ CD8 gating by excluding dead cells, CD14+, CD19+, and CD16+ cells. For intracellular cytokine staining (ICS), the cytokine positive/ negative population were gated according to corresponding negative controls, known as unstimulated samples. For ICS, following live CD3+ T cells gating, cells then were gated into CD8+ T cells (CD8+CD4-)and CD4+ T cells (CD4+CD8); IFN-g +/-, TNFa+/-, IL-2+/- and CD107a+/- populations were gated in consistence with the corresponding negative controls. For Pentamer phenotyping experiments, following live CD3+ T cells gating, cells were gated on CD8+ Pentamer+population. These cells were then analyzed for percentage expression of a particular marker using unstained and overall CD8+ populations to determine where to place the gates. Fluorescence minus one (FMO) control samples were also applied to determine positive and negative populations.

☒ Tick this box to confirm that a figure exemplifying the gating strategy is provided in the Supplementary Information.